Science Advances

AAAS

advances.sciencemag.org/cgi/content/full/3/6/e1601667/DC1

Supplementary Materials for

Fully gapped superconductivity with no sign change in the prototypical heavy-fermion $CeCu_2Si_2$

Takuya Yamashita, Takaaki Takenaka, Yoshifumi Tokiwa, Joseph A. Wilcox, Yuta Mizukami, Daiki Terazawa, Yuichi Kasahara, Shunichiro Kittaka, Toshiro Sakakibara, Marcin Konczykowski, Silvia Seiro, Hirale S. Jeevan, Christoph Geibel, Carsten Putzke, Takafumi Onishi, Hiroaki Ikeda, Antony Carrington, Takasada Shibauchi, Yuji Matsuda

Published 23 June 2017, *Sci. Adv.* **3**, e1601667 (2017)
DOI: 10.1126/sciadv.1601667

This PDF file includes:

section S1. Temperature dependence of penetration depth

The data for the temperature dependence of the penetration depth $\Delta\lambda(T)$ measured in two samples show consistent results (fig. S1), which can be fitted to the exponential dependence expected for the fully gapped superconductors.

In fig. S2, the T-exponent n of the $\Delta\lambda(T)$ data in the power-law fit and the effective gap Δ_e in the exponential fit are plotted as a function of the upper limit of the fit, $T_{\max}$. In clean and dirty d-wave superconductors (or more generally superconductors with line nodes) power-law dependencies with exponents 1 and 2 are expected (fig. S2A, dashed lines). In a multigap system the effective gap Δ_e is close to the minimum one on all sheets of Fermi surface.

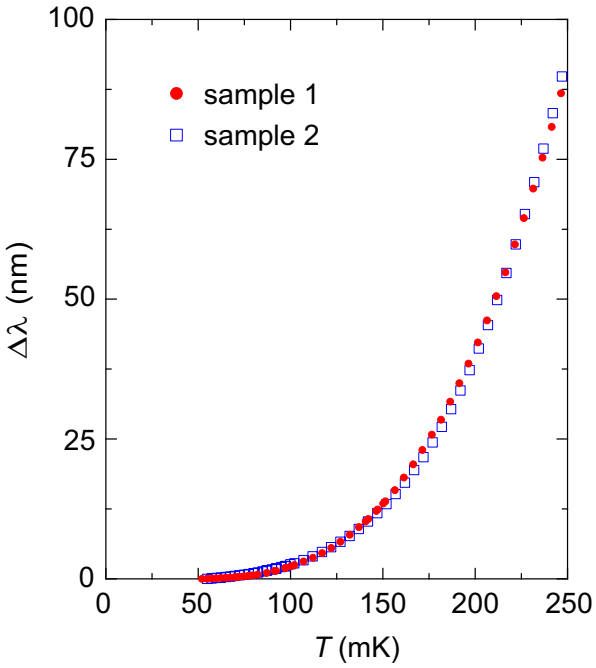

fig. S1. **Magnetic penetration depth versus temperature for two samples measured.** Sample 1 is the same as show in Fig. 3B. The data for sample 2 have been multiplied by 1.16 for comparison to sample 1. The temperature dependence is almost identical but the scale factors differ by 20% which is within the bound of the expected error on the geometrical scale factors.

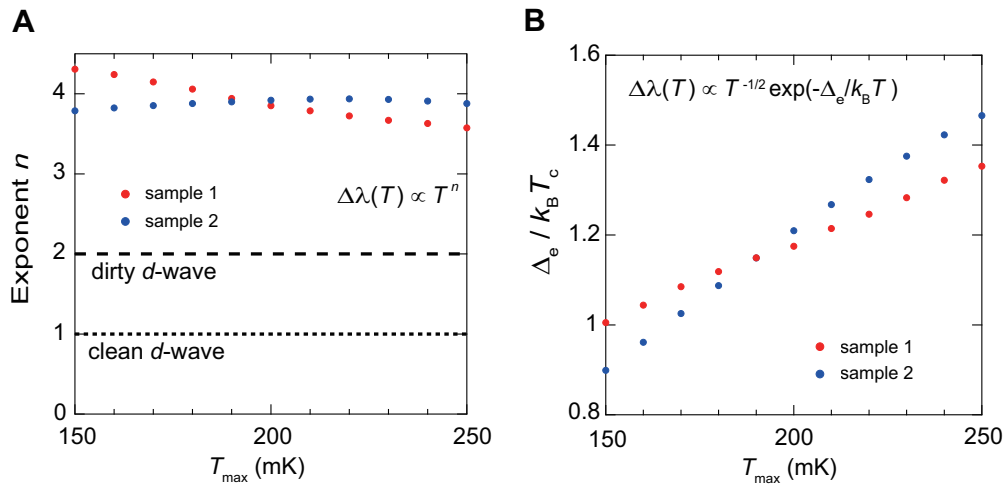

fig. S2. **Parameters obtained for the fits to the $\Delta\lambda(T)$ data.** (**A** and **B**) The low-temperature penetration depth data are fitted by using the power-law T^n (**A**) and exponential temperature dependence $T^{-1/2}\exp(-\Delta_e/k_BT)$ (**B**), where the fitting temperature range is chosen up to the maximum temperature T_{max}.

section S2. Lower critical field

Our radio-frequency inductive measurements measure very precisely the temperature dependence of the magnetic penetration depth λ relative to some reference level at low temperature, but not its absolute value. To determine the absolute value we have performed measurements of the lower critical field H_{c1} using a micro-Hall probe array. An array of Hall sensors is placed below the sample and so the magnetic induction B at the position of the Hall sensor is measured as a function of the applied field H. Figure S3 shows a $B(H)$ curve for a Hall sensor close to the center of a sample of $CeCu_2Si_2$ of approximate dimensions $0.29\times0.40\times0.09\,\mathrm{mm}^3$. At each temperature the sample was cooled in nominally zero field and the field increased towards the maximum. The sample was then warmed above T_c and cooled again in zero field and the field increased towards the negative limit. The magnetic field was produced by a copper solenoid so the remnant field from this was very low but the earth's field was not shielded. Tests showed that cooling in a small (positive or negative) field of less than 0.1 mT did not change the results.

At low field there is a small linear increase in B with H because of incomplete flux shielding of the sensor by the sample which sits a few microns above. At a well-defined field

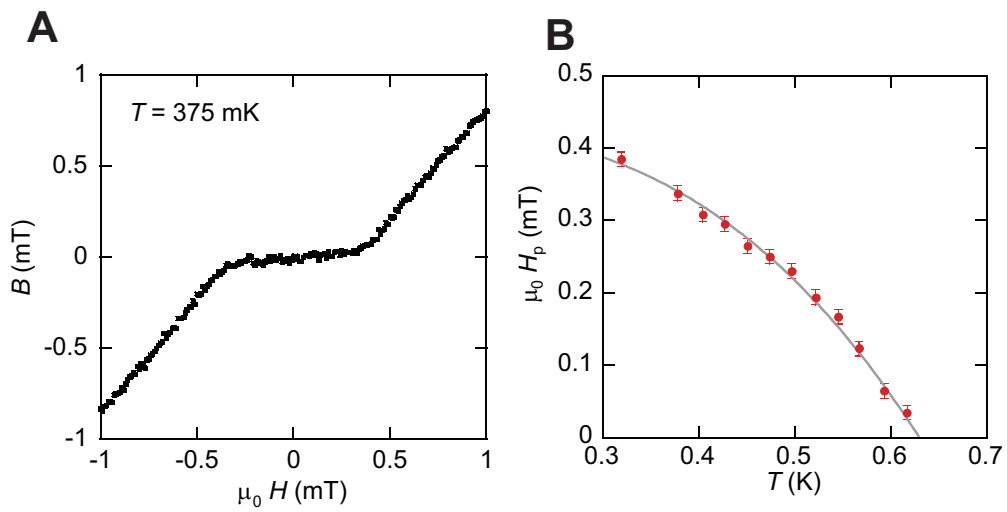

fig. S3. **Lower-critical field measurements of $CeCu_2Si_2$.** (**A**) Magnetic induction (B) versus applied field (H) measured by a Hall sensor a few microns below the middle of the sample. Two sweeps are shown, one for increasing field and another for decreasing field. The sample was zero field cooled before each sweep. (**B**) Field of first flux penetration H_p versus temperature. The line is a guide to the eye.

H_p flux enters the sample and B increases rapidly with increasing H. Taking the average of H_p for the positive and negative field sweeps cancels out the offset due to the earth's field. We relate H_p to H_{c1} using the following relation from Brandt [52] for a strip

$$\frac{H_p}{H_{c1}} = \tanh\sqrt{\frac{0.36c}{a}}$$

where a is the shorter of the in-plane dimensions of the sample and c is the c-axis dimension (our measurements are performed with $B \parallel c$). At $T = 320\,\mathrm{mK}$ we find $H_p = 0.39\,\mathrm{mT}$ and $H_{c1} = 1.2 \pm 0.1\,\mathrm{mT}$, where the error includes uncertainty in the sample dimensions. Then solving the Ginzburg-Landau equation

$$\mu_0 H_{c1} = \frac{\phi_0}{4\pi\lambda^2}\left[\ln\left(\frac{\lambda}{\xi}\right) + 0.5\right]$$

with $\xi = 4.7\,\mathrm{nm}$, gives $\lambda(T = 320\,\mathrm{mK}) = 890 \pm 40\,\mathrm{nm}$. Then we use the radio frequency measured change in λ from 50 mK to 320 mK, $\Delta\lambda = 190 \pm 25\,\mathrm{nm}$, to calculate $\lambda(T = 0) = 700 \pm 50\,\mathrm{nm}$. Repeating this procedure for a second sample, with dimensions $0.35 \times 0.32 \times 0.041\,\mathrm{mm}^3$, gave a consistent result within the error, $\lambda(T = 0) = 680 \pm 50\,\mathrm{nm}$.

section S3. Zero-field thermal conductivity

The thermal conductivity in the superconducting state can be written as a sum of the quasiparticle and phonon contributions, $\kappa = \kappa_{\rm qp} + \kappa_{\rm ph}$. The phonon conductivity in the boundary-limited scattering regime at low temperature is expressed as, $\kappa_{\rm ph} = \frac{1}{3}\beta\langle v_s\rangle\ell_{\rm ph}T^3$, where β is the phonon specific heat coefficient, $\langle v_s\rangle$ is the mean acoustic phonon velocity, and $\ell_{\rm ph}$ is the phonon mean free path. At low temperatures, $\kappa_{\rm ph}$ shows a power-law dependence on temperature; $\kappa_{\rm ph} \propto T^{\alpha}$ and α ranges from 2 to 3, depending on the nature of the surface scattering. In real systems, α takes a value intermediate between 2 and 3 [53]. The best fit in a wide T-range is obtained for $\alpha = 2.4$ for κ_a. In this case, the residual term is close to zero (fig. S4B).

For comparison, we show κ/T plotted against T, $T^{1.4}$ and T^2 in fig. S4. When κ/T is plotted against T, a linear extrapolation to zero temperature results in an unphysical negative value. Moreover, κ/T deviates from the fit at the lowest temperature. When κ/T is plotted against $T^{1.4}$ as shown in the middle panel, it is linearly fitted up to 0.2 K without deviation at low temperature. The right panel shows κ/T plotted against T^2. The data exhibit a convex curvature, indicating that κ/T does not follow a T^2 dependence.

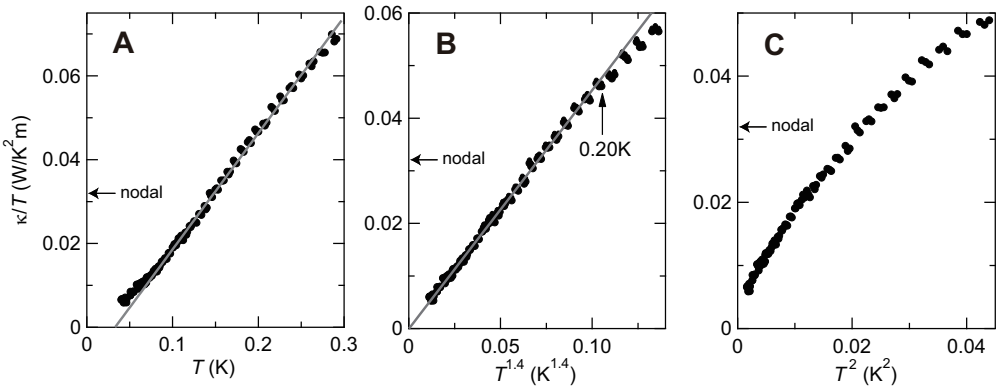

fig. S4. **Temperature dependence of thermal conductivity at low temperatures.** (**A**) Thermal conductivity divided by temperature κ/T of $CeCu_2Si_2$ plotted against T for heat current along the a-axis in zero field. (**B**) The same data of κ/T plotted against $T^{1.4}$. (**C**) The same data plotted against T^2. Solid lines are linear fits to the data. The arrow in the middle panel marks the temperature where the fits starts to deviate from the linear behavior. The value of κ/T expected for a line nodes is indicated.

In a superconductor with line nodes, a finite residual thermal conductivity $\kappa_0/T \equiv \kappa/T(T \to 0\,\mathrm{K})$ is expected due to the existence of a residual normal fluid, which is a consequence of impurity scattering, even for low concentrations of non-magnetic impurities [54]. At $T = 40\,\mathrm{mK}$, in-plane phonon conductivity κ_a^{ph}/T estimated by using the Wiedemann-Franz law in the normal state, $\kappa_a^{\mathrm{ph}}/T = \kappa_a(H_{c2})/T - L_0/\rho_a(T)$, is $\sim 4\,\mathrm{mW/K^2m}$, which yields in-plane quasiparticle thermal conductivity $\kappa_a^{\mathrm{qp}}/T \sim 3\,\mathrm{mW/K^2m}$ in zero field. The residual thermal conductivity expected for line node is estimated as $\kappa_{a0}/T \approx (L_0/\rho_{a0}) \cdot (\xi_{ab}/\ell_{ab}) \sim 32\,\mathrm{mW/K^2m}$ [54]. Here $\xi_{ab} = 4.7\,\mathrm{nm}$ is the in-plane coherence length estimated by the orbital limited upper critical field of 14.7 T for $\mathbf{H} \parallel c$ [20] and $\ell_{ab} \sim 8\,\mathrm{nm}$ is the in-plane mean free path obtained from $\ell_{ab} = v_F^{ab}\lambda^2(0)\mu_0/\rho_{a0}$, using $\rho_{a0} = 43\,\mu\Omega\mathrm{cm}$ and the average of in-plane Fermi velocity $v_F^{ab} \sim 5800\,\mathrm{m/s}$ for the hole band calculated by LDA+U, taking into account the mass renormalization $z = 1/50$ which is determined by the specific heat measurements. These results indicate that the residual thermal conductivity at $T \to 0\,\mathrm{K}$, if present, is considerably smaller than that expected for line node (fig. S4). A similar conclusion is obtained for the out-of-plane thermal conductivity κ_c ($\mathbf{Q} \parallel c$).